

# Desymmetrization of Cyclohexanes by Site- and Stereoselective C–H Functionalization

Jiantao Fu,<sup>1</sup> Zhi Ren,<sup>1</sup> John Bacsa,<sup>1</sup> Djamaladdin G. Musaev<sup>1,2</sup> & Huw M. L. Davies<sup>1\*</sup>

<sup>1</sup>Department of Chemistry, Emory University, 1515 Dickey Drive, Atlanta, Georgia 30322

<sup>2</sup>Cherry L. Emerson Center for Scientific Computation, Emory University, 1521 Dickey Drive, Atlanta, Georgia 30322

9 Abstract: C–H bonds have long been considered as generally unreactive, but new  
10 methods are being continually developed to transform these bonds that are  
11 otherwise inert to traditional chemical reagents.<sup>1–9</sup> The challenge, however, is to  
12 achieve such transformations in a highly selective manner, especially if the C–H  
13 bonds are unactivated<sup>10</sup> or not adjacent to a directing group.<sup>11–13</sup> Having catalyst-  
14 controlled site-selectivity, whereby the natural tendencies of the substrates<sup>14</sup> can  
15 be overwhelmed simply by choosing an appropriate catalyst, is a very attractive  
16 concept. Therefore, substantial effort has been made in catalyst-controlled C–H  
17 functionalization.<sup>6, 15–17</sup> In particular, methylene C–H bond functionalization has  
18 attracted wide scientific interest, and while several new methods have targeted  
19 these bonds in cyclic alkanes, the levels of selectivity were relatively poor.<sup>18–20</sup>  
20 Here, we illustrate a new level of sophistication in catalyst-controlled C–H  
21 functionalization, in which unactivated cyclohexane derivatives can be  
22 desymmetrized in a highly site- and stereoselective manner through  
23 donor/acceptor carbene insertion.

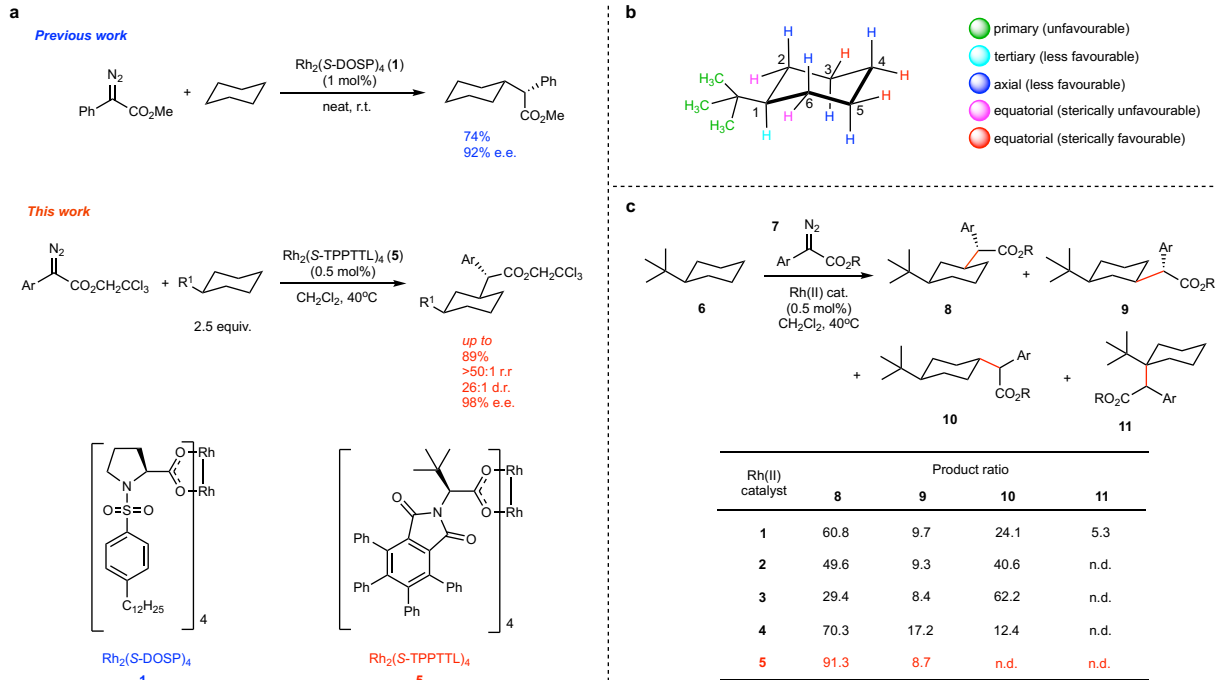
25 Selective reactions on certain cyclohexanes or polycyclic systems with appropriately  
 26 positioned deactivating functionalities have been achieved.<sup>18-22</sup> However, in simple,  
 27 electronically neutral cyclohexanes, good control of site- and stereoselectivity remains  
 28 an unsolved challenge. Representative strategies in this area include carbene-induced  
 29 C–H insertion,<sup>23</sup> C–H oxidation,<sup>18</sup> and radical-induced C–H functionalizations,<sup>20-21, 24</sup>  
 30 although they have achieved limited levels of selectivity. Therefore, the principal

31 challenge of achieving these C–H functionalization processes in a highly site- and  
32 stereoselective fashion has not been satisfactorily addressed.

33  
34 Our group has reported the design and development of a series of chiral dirhodium  
35 catalysts (**1–5**) with different steric environments (Fig. 1a and Extended Data Fig. 1).  
36 These catalysts are effective at catalyzing C–H functionalization reactions of acyclic  
37 alkanes via donor/acceptor carbene insertion.<sup>6, 10, 15, 25</sup> We have also described the  
38 functionalization of cyclohexane using  $\text{Rh}_2(\text{S-DOSP})_4$  (**1**) (Fig. 1a).<sup>10</sup> As the next  
39 challenge for our Rh(II)-catalyzed C–H functionalization program and with the recent  
40 development of 2,2,2-trichloroethyl aryldiazoacetates as a more robust source of  
41 donor/acceptor carbenes,<sup>26</sup> we became intrigued with the possibility of achieving site  
42 selective C–H functionalization of more elaborate substrates, such as substituted  
43 cyclohexanes. In this paper, we describe the development and evaluation of a new  
44 dirhodium catalyst,  $\text{Rh}_2(\text{S-TPPTL})_4$  (**5**), leading to a site-selective carbene insertion  
45 process with high asymmetric induction. In particular, a higher level of sophistication in  
46 stereocontrol is achieved, as the reaction generates three stereocenters in one step  
47 from an achiral substrate. For monosubstituted cyclohexanes, the catalyst is not only  
48 able to differentiate between C-3 and C-4, but also between C-3 and C-5, leading to  
49 desymmetrization of the substrate and generation of the products with high  
50 diastereoselectivity and enantioselectivity (Fig. 1).

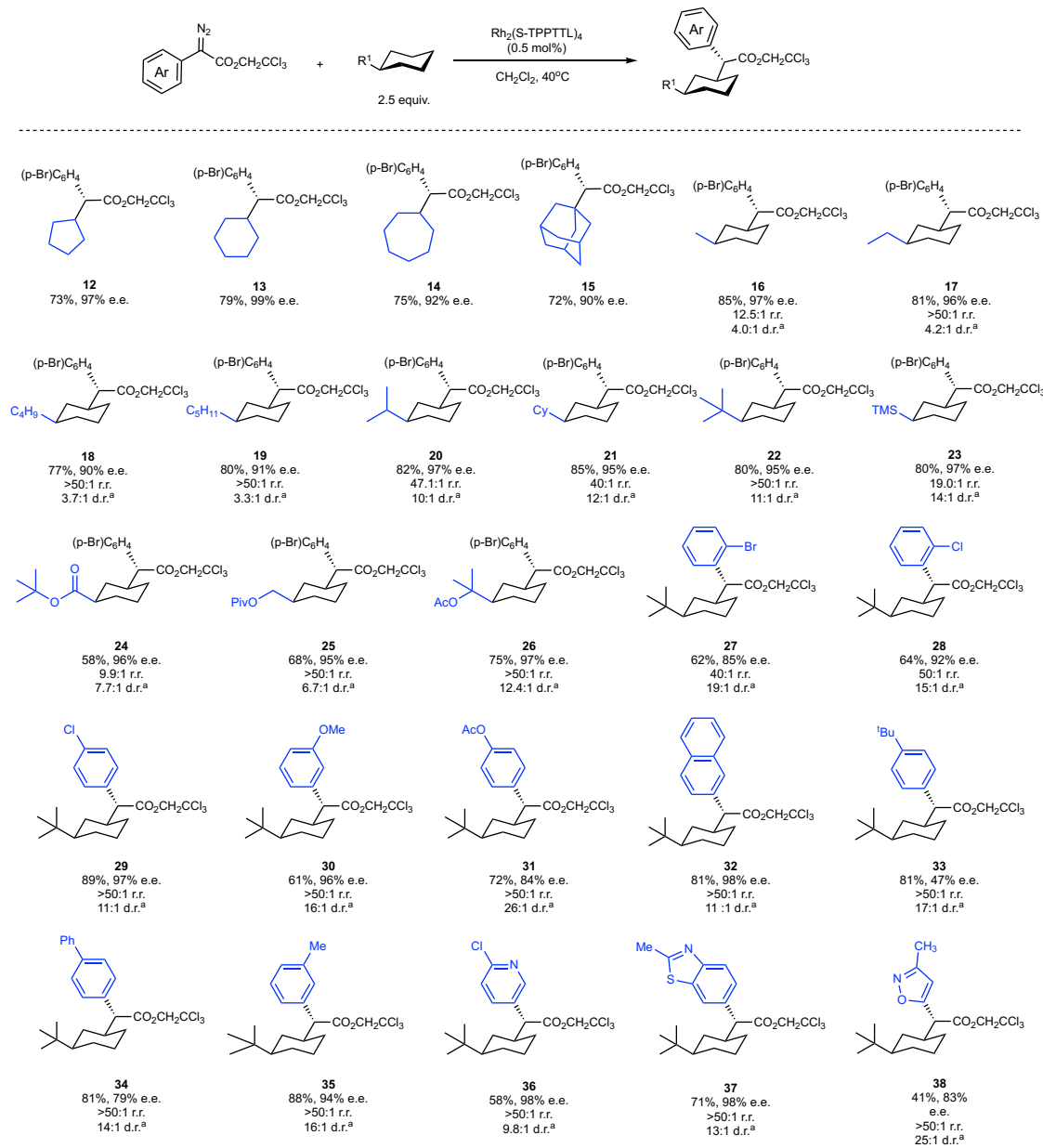
51  
52 We first examined *tert*-butylcyclohexane as our model substrate. With the bulky *tert*-  
53 butyl group preferentially in equatorial position, there exist 11 different C–H bonds,  
54 excluding primary ones, that are electronically favored toward C–H functionalization  
55 (Fig. 1b). The C-1 axial position may be accessible for a structurally flexible catalyst but  
56 still largely unfavored due to steric reasons. In addition, C–H bonds at C-2 and C-6  
57 positions are likely to be too crowded for functionalization due to steric bulk of the  
58 rhodium carbene. For similar considerations, equatorial C–H bonds are more favored  
59 than their axial counterparts. Therefore, it is reasonable to expect that three sites would  
60 be most favorable: the equatorial C–H bonds at C-3, C-4, and C-5 (marked in red, Fig.  
61 1b).

62 Initial exploratory studies of the reaction were conducted using 2,2,2-trichloroethyl 2-(4-  
63 bromophenyl)-2-diazoacetate (**7**) as the carbene source. When the relatively uncrowded  
64 catalyst,  $\text{Rh}_2(\text{S-DOSP})_4$  (**1**) was used, the reaction gave primarily a mixture of three  
65 methylene insertion products **8-10** with a small but noticeable quantity of C-1 methine  
66 insertion product **11**. Catalysts **2-4** were sufficiently sterically hindered to block methine  
67 insertion, but still gave a mixture of products **8-10** (entries 2-4, Fig. 1c). During the  
68 course of these studies we evaluated a range of other established catalysts (see  
69 Supplementary Information section 3 for complete optimization study), as well as the  
70 new catalyst,  $\text{Rh}_2(\text{S-TPPTTL})_4$ , which was readily prepared on multi-gram scale in two  
71 steps.  $\text{Rh}_2(\text{S-TPPTTL})_4$  has not been reported previously, even though it is structurally  
72 related to  $\text{Rh}_2(\text{S-TCPTAD})_4$ <sup>6</sup> and other phthalimido-based catalysts developed by  
73 Hashimoto.<sup>27-30</sup> We were pleased to discover that, in contrast to all the previous  
74 catalysts we had studied,  $\text{Rh}_2(\text{S-TPPTTL})_4$  gave a very clean reaction (entry 5, Fig. 1c),  
75 favoring predominately a single methylene C–H functionalization product (**8**) with high  
76 site selectivity (>50:1 r.r.) and asymmetric induction (95% e.e.) (see Supplementary  
77 Information section 7 for X-ray structure of **8**). Notably, the product derived from C-4  
78 insertion (**10**) was not seen in the reaction catalyzed by  $\text{Rh}_2(\text{S-TPPTTL})_4$ . The products  
79 **8** and **9** are diastereomers and are formed through a desymmetrization event, and  
80 therefore, this catalyst effectively distinguishes between C-3 and C-4, and between the  
81 enantiotopic equatorial hydrogens at C-3 and C-5, which have not been reported  
82 previously for any C–H functionalization of alkyl cyclohexanes.



Having established that  $\text{Rh}_2(\text{S-TPPTTL})_4$  is the optimal catalyst, we then sought to explore the reaction with other cycloalkanes (Fig. 2). Simple cycloalkanes were readily functionalized to produce **12-15** in good yield (73-79% yield) and high enantioselectivity (90-99% e.e.). With these benchmark data, we then explored a series of alkyl cyclohexanes to study the influence of the size of the substituent. All substrates underwent functionalization at the desired C-3 position to form **16-22** with very high site selectivity, although in a few cases regioisomers were observed in minute amounts in the crude reaction mixture. Excellent levels of enantioselectivity ( $\geq 90\%$  e.e.) were achieved for these substrates, indicating that  $\text{Rh}_2(\text{S-TPPTTL})_4$  routinely gives high asymmetric induction at the carbene site. Particularly notable compounds are **18** and **19**, because regioisomers derived from possible reactions at the alkyl chains were formed only in trace amounts ( $>50:1$  r.r.), even though these C-H bonds are very accessible. The levels of diastereoselectivity were about 4:1 d.r. when the substituent was methyl or primary (**16-19**), but steadily improved when it was secondary or tertiary (**20-22**, 10-12:1 d.r.). These results indicate that the desymmetrization is more pronounced as the size of the alkyl substituent increases. Replacing the *tert*-butyl group in the model substrates with trimethylsilyl (TMS) group led to minimal change of reaction outcome (**23**). Furthermore, cyclohexanes bearing various ester groups also underwent

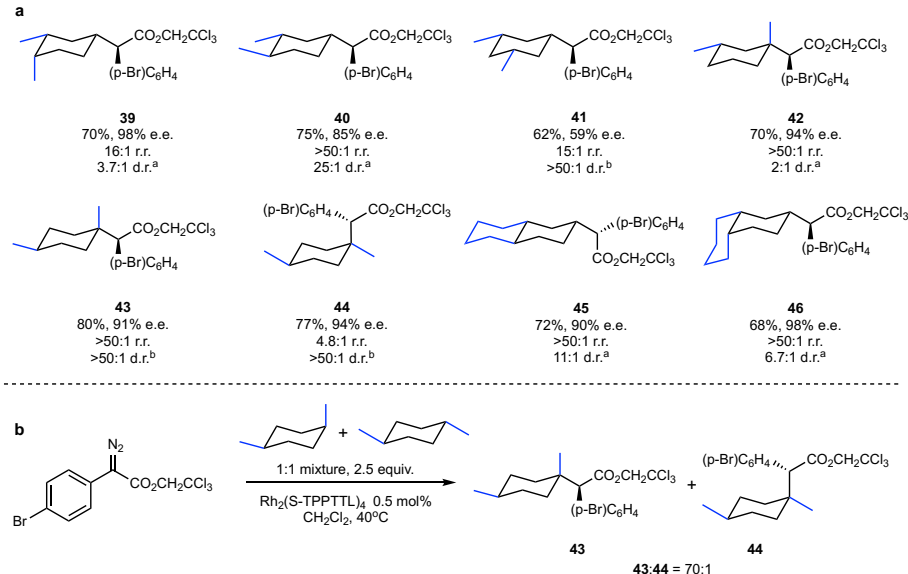
102 clean functionalization to generate products **24-26** with good regio- and stereocontrol. In  
 103 addition, the reaction was compatible with a variety of aryl diazoacetates, including some  
 104 that contain heteroaryl donor groups (**27-38**). However, the level of asymmetric  
 105 induction is somewhat sensitive to the steric bulk of the *para* substituent of the aryl  
 106 group, as **33** and **34** were generated with high diastereoselectivity but lower  
 107 enantioselectivity (47% and 79% e.e. respectively).



108  
 109 The selectivity of C–H functionalization by rhodium carbene is generally considered to  
 110 be governed by a combination of steric and electronic influences of the substrate and

111 the catalyst of choice.<sup>10, 15, 25</sup> Attempting to further evaluate these selectivity principles  
112 and to test the catalyst in more complex systems, we also subjected disubstituted alkyl  
113 cyclohexanes to the C–H functionalization reaction (Fig. 3). *cis*-1,2-  
114 Dimethylcyclohexane and *trans*-1,3-dimethylcyclohexane are interesting substrates  
115 because they exist as a 1:1 mixture of enantiomeric chair forms. Both substrates were  
116 capable of effective C–H functionalization, generating the products **39** and **42** with  
117 moderate to high level of asymmetric induction (98% and 59% e.e.). However, the  
118 diastereoselectivity in the formation of **39** and **42** is quite low (2.2–3.7:1 d.r.), indicating  
119 that the reaction was occurring with both enantiomeric chair forms for the substrates.  
120 *trans*-1,2-Dimethylcyclohexane is chiral and was reacted as the racemate mixture. Even  
121 so, the reaction was very effective, generating **40** with excellent site- and  
122 stereoselectivity. In addition, *trans*- and *cis*-1,4-dimethylcyclohexane are interesting  
123 substrates because they allow an evaluation of the difference in reactivity between an  
124 axial and an equatorial C–H bond. Reaction with *cis*-1,4-dimethylcyclohexane resulted  
125 in C–H functionalization into a tertiary C–H site to form **43**. *trans*-1,4-  
126 Dimethylcyclohexane would be expected to exist primarily in the chair form with the two  
127 methyl groups in equatorial positions, yet this substrate is also capable of C–H  
128 functionalization to form **44**. However, the regioselectivity is lower (4.3:1 r.r.),  
129 presumably due to unfavored axial insertion and competition at other methylene sites. A  
130 substrate competition experiment using an equal mixture of both 1,4-  
131 dimethylcyclohexane isomers indicated that an equatorial C–H bond reacted  
132 approximately 140 times faster than an axial C–H bond (see Supplementary Information  
133 section 3 for experimental details). The equatorial preference observed here is much  
134 higher than what has been seen in other C–H functionalization reactions.<sup>23, 24</sup> Finally,  
135 the study was extended to *cis*- and *trans*-decalin and they also gave clean  
136 transformations, forming **45** and **46** with excellent regio- and stereocontrol. The  
137 structure of **45** was confirmed by X-ray crystallography (see Supplementary Information  
138 section 7).

139



140  
141

142 In order to understand what features of  $\text{Rh}_2(\text{S-TPPTTL})_4$  make it such an exceptional  
143 catalyst for the desymmetrization of cyclohexanes, the structure of the catalyst was  
144 interrogated by X-ray crystallography and by DFT calculations (see Supplementary  
145 Information section 6 and 7 for details). The X-ray data indicate that the catalyst  
146 comprises a dirhodium core and four phthalimido groups with the four S-TPPTTL  
147 ligands that adopt a “chiral crown” shape,<sup>29</sup> slightly distorted from a perfect C<sub>4</sub>  
148 symmetric structure (Fig. 4), and is similar to other phthalimido dirhodium catalysts.<sup>6, 29</sup>  
149 The flanking phthalimido groups are projected upward in relation to the dirhodium core,  
150 embedding an approximate C<sub>4</sub> symmetry on the macrocycle. A unique structural feature  
151 of  $\text{Rh}_2(\text{S-TPPTTL})_4$  is the orientation of the 16 phenyl groups bound to the phthalimido  
152 ligands. The X-ray crystallographic structure of  $\text{Rh}_2(\text{S-TPPTTL})_4$  shows that twelve of  
153 the phenyl groups are tilted to the right and four are tilted in the opposite direction.  
154 Further computational studies indicate that structure **47b** with all the phenyl groups tilted  
155 to the right (*M* configuration) is lower in energy by 2.9 kcal/mol than structure **47a**.  
156 Closer inspection of the structure reveals that the *tert*-butyl group of one ligand  
157 influences the tilt direction of the phenyl rings on the adjacent ligand. Indeed, attempts  
158 at calculating the energy of the complex with all the phenyl groups tilted to the left were  
159 not successful because the structure reverted back to the *M* configuration (see  
160 Supplementary Information section 6 for details). Thus, the point chirality of the ligands  
161 induces a pseudo C<sub>4</sub> propeller chirality in the complex by causing the sixteen phenyl

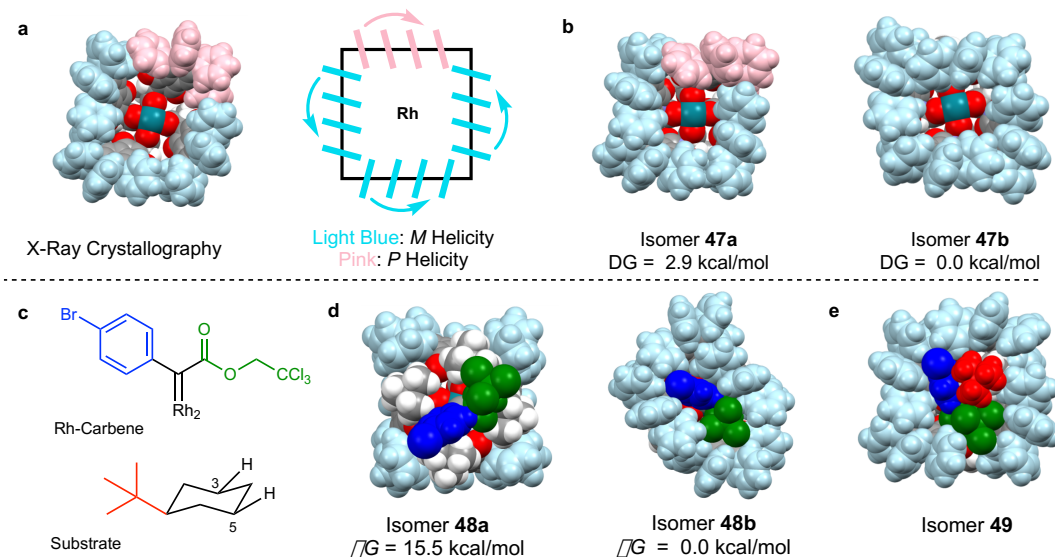
162 groups to tilt preferentially in one direction over the other. We propose that the  
163 orientations of these phenyl groups play a critical role in the observed selectivities.

164

165 Even though the ligands generate a deep pocket around the rhodium, computational  
166 studies indicate that binding of the carbene to this face (structure **48b**) is strongly  
167 preferred by 15.5 kcal/mol in energy as compared to structure **48a**, presumably  
168 because of the steric influence of the four *tert*-butyl groups. In structure **48b**, all phenyl  
169 groups are tilted in the same direction, and its other isomers, including the one with two  
170 oppositely tilted ligands, are higher in energy (see Supplementary Information section 6  
171 for details). Interestingly, comparison between the free catalyst (**47b**) and carbene-  
172 bound catalyst (**48b**) structures reveals that the overall shape of the ligand framework  
173 has changed to accommodate the carbene, indicative of an induced fit model.

174

175 The next stage of the computational study was to understand how *tert*-butylcyclohexane  
176 approaches the rhodium carbene. We therefore calculated several isomers of the Rh-  
177 (carbene)(substrate) complexes.<sup>30</sup> These studies reveal that attack at the C-4 position  
178 of the cyclohexane was very unfavorable because the *tert*-butyl group would be pointing  
179 toward the “wall” of the catalyst, generated by the 16 phenyl groups. The most favorable  
180 structure of the Rh-(carbene)(substrate) complex is **49**, where the *tert*-butyl group is  
181 pointing away from the “wall” of the pocket, toward the opening of the binding face. This  
182 places one of the enantiotopic equatorial C-3 hydrogens close to the carbene, leading to  
183 the correct prediction of the observed asymmetric induction during desymmetrization.  
184 Examination of structure **49** shows that the shape of the catalyst has adjusted once  
185 again to accommodate the substrate. Overall, these calculations show that Rh<sub>2</sub>(S-  
186 TPPTTL)<sub>4</sub> has a high degree of flexibility to adjust its shape when the carbene and  
187 substrate approach the catalytically active rhodium center, which may explain why the  
188 reaction can be extended to disubstituted cyclohexanes and decalins.



189  
190

191 In conclusion, this study serves to demonstrate that catalyst-controlled C–H  
192 functionalization of substituted cyclohexanes in a site- and stereoselective manner is a  
193 viable process. This study also further underscores the subtle controlling influences in  
194 the C–H functionalization reactions of donor/acceptor carbenes in the presence of  
195 appropriately designed dirhodium catalysts.

196  
197

## References

- Yamaguchi, J.; Yamaguchi, A. D. & Itami, K. C–H bond functionalization: emerging synthetic tools for natural products and pharmaceuticals. *Angew. Chem. Int. Ed.* **51**, 8960–9009 (2012).
- Davies, H. M. L. & Morton, D. Recent advances in C–H functionalization. *J. Org. Chem.* **81**, 343–350 (2016).
- Gutekunst, W. R. & Baran, P. S. C–H functionalization logic in total synthesis. *Chem. Soc. Rev.* **40**, 1976–1991 (2011).
- Wencel-Delord, J. & Glorius, F. C–H bond activation enables the rapid construction and late-stage diversification of functional molecules. *Nat. Chem.* **5**, 369–375 (2013).
- Fier, P. S. & Hartwig, J. F. Synthesis and late-stage functionalization of complex molecules through C–H fluorination and nucleophilic aromatic substitution. *J. Am. Chem. Soc.* **136**, 10139–10147 (2014).
- Liao, K.; Pickel, T. C.; Boyarskikh, V.; Bacsa, J.; Musaev, D. G. & Davies, H. M. L. Site-selective and stereoselective functionalization of non-activated tertiary C–H bonds. *Nature* **551**, 609–613. (2017).
- McMurray, L.; O'Hara, F. & Gaunt, M. J. Recent developments in natural product synthesis using metal-catalysed C–H bond functionalisation. *Chem. Soc. Rev.* **40**, 1885–1898 (2011).
- Newhouse, T. & Baran, P. S. If C–H bonds could talk: selective C–H bond oxidation. *Angew. Chem. Int. Ed.* **50**, 3362–3374 (2011).
- Davies, H. M. L. & Manning, J. R. Catalytic C–H functionalization by metal carbenoid and nitrenoid insertion. *Nature* **451**, 417–424 (2008).
- Davies, H. M. L.; Hansen, T. & Churchill, M. R. Catalytic asymmetric C–H activation of alkanes and tetrahydrofuran. *J. Am. Chem. Soc.* **122**, 3063–3070 (2000).

220 11. He, J.; Wasa, M.; Chan, K. S. L.; Shao, Q. & Yu, J. Q. Palladium-catalyzed transformations of alkyl  
221 C–H bonds. *Chem. Rev.* **117**, 8754–8786 (2017).

222 12. Colby, D. A.; Bergman, R. G. & Ellman, J. A. Rhodium-catalyzed C–C bond formation via  
223 heteroatom-directed C–H bond activation. *Chem. Rev.* **110**, 624–655 (2010).

224 13. Hartwig, J. F.; Larsen, M. A. Undirected, homogeneous C–H bond functionalization: challenges and  
225 opportunities. *ACS Cent. Sci.* **2**, 281–292 (2016).

226 14. Davies, H. M. & Morton, D. Guiding principles for site selective and stereoselective intermolecular C–  
227 H functionalization by donor/acceptor rhodium carbenes. *Chem. Soc. Rev.* **40**, 1857–1869 (2011).

228 15. Liao, K.; Negretti, S.; Musaev, D. G.; Bacsa, J. & Davies, H. M. L. Site-selective and stereoselective  
229 functionalization of unactivated C–H bonds. *Nature* **533**, 230–234 (2016).

230 16. Qin, C.; Boyarskikh, V.; Hansen, J. H.; Hardcastle, K. I.; Musaev, D. G.; Davies, H. M. L. D2-  
231 Symmetric Dirhodium Catalyst Derived from a 1,2,2-Triaryl(cyclopropanecarboxylate Ligand: Design,  
232 Synthesis and Application. *J. Am. Chem. Soc.* **133**, 19198–19204 (2011).

233 17. Qin, C. & Davies H. M. L. Role of sterically demanding chiral dirhodium catalysts in site-selective C–  
234 H functionalization of activated primary C–H bonds. *J. Am. Chem. Soc.* **136**, 9792–9796 (2014).

235 18. Chen, M. S. & White, M. C. Combined effects on selectivity in Fe-catalyzed methylene oxidation.  
236 *Science* **327**, 566–571 (2010).

237 19. Czaplyski, W. L.; Na, C. G. & Alexanian, E. J. C–H Xanthylation: a synthetic platform for alkane  
238 functionalization. *J. Am. Chem. Soc.* **138**, 13854–13857 (2016).

239 20. Schmidt, V. A.; Quinn, R. K.; Brusoe, A. T. & Alexanian, E. J. Site-selective aliphatic C–H  
240 bromination using *N*-bromoamides and visible light. *J. Am. Chem. Soc.* **136**, 14389–14392 (2014).

241 21. Quinn, R. K.; Konst, Z. A.; Michalak, S. E.; Schmidt, Y.; Szklarski, A. R.; Flores, A. R.; Nam, S.;  
242 Horne, D. A.; Vanderwal, C. D. & Alexanian, E. J. Site-selective aliphatic C–H chlorination using *N*-  
243 chloroamides enables a synthesis of chlorolissoclimide. *J. Am. Chem. Soc.* **138**, 696–702 (2016).

244 22. Wasa, M.; Chan, K. S.; Zhang, X. G.; He, J.; Miura, M. & Yu, J. Q. Ligand-enabled methylene C(sp<sup>3</sup>)-  
245 H bond activation with a Pd(II) catalyst. *J. Am. Chem. Soc.* **134**, 18570–18572 (2012).

246 23. Chen, K.; Eschenmoser, A. & Baran, P. S. Strain release in C–H bond activation? *Angew. Chem. Int.*  
247 *Ed.* **48**, 9705–9708 (2009).

248 24. Dondi, D.; Ravelli, D.; Fagnoni, M.; Mella, M.; Molinari, A.; Maldotti, A. & Albini, A. Regio- and  
249 stereoselectivity in the decatungstate photocatalyzed alkylation of alkenes by alkylcyclohexanes.  
250 *Chem. Eur. J.* **15**, 7949–7957 (2009).

251 25. Liao, K.; Yang, Y.; Li, Y.; Sanders, J. N.; Houk, K. N.; Musaev, D. G. & Davies, H. M. L. Design of  
252 catalysts for site-selective and enantioselective functionalization of non-activated primary C–H  
253 bonds. *Nat. Chem.* **10**, 1048–1055 (2018).

254 26. Guptill, D. M. & Davies, H. M. L. 2,2,2-Trichloroethyl aryldiazoacetates as robust reagents for the  
255 enantioselective C–H functionalization of methyl ethers. *J. Am. Chem. Soc.* **136**, 17718–17721  
256 (2014).

257 27. Saito, H.; Oishi, H.; Kitagaki, S.; Nakamura, S.; Anada, M. & Hashimoto, S. Enantio- and  
258 diastereoselective synthesis of cis-2-aryl-3-methoxycarbonyl-2,3-dihydrobenzofurans via the Rh(II)-  
259 Catalyzed C–H Insertion Process. *Org. Lett.* **4**, 3887–3890 (2002).

260 28. Kitagaki, S.; Anada, M.; Kataoka, O.; Matsuno, K.; Umeda, C.; Watanabe, N. & Hashimoto, S.-I.  
261 Enantiocontrol in tandem carbonyl ylide formation and intermolecular 1,3-dipolar cycloaddition of  $\alpha$ -  
262 diazo ketones mediated by chiral dirhodium(II) carboxylate catalyst. *J. Am. Chem. Soc.* **121**, 1417–  
263 1418 (1999).

264 29. DeAngelis, A.; Boruta, D. T.; Lubin, J. B.; Plampin, J. N., 3rd; Yap, G. P. & Fox, J. M. The chiral  
265 crown conformation in paddlewheel complexes. *Chem. Commun.* **46**, 4541–4543 (2010).

266 30. Nakamura, E.; Yoshikai, N.; Yamanaka, M. Mechanism of C–H Bond Activation/C–C Bond  
267 Formation Reaction between Diazo Compound and Alkane Catalyzed by Dirhodium  
268 Tetra carboxylate. *J. Am. Chem. Soc.* **124**, 7181–7192 (2002).

269

270 **Acknowledgements:** Financial support was provided by NSF under the CCI Center for  
271 Selective C–H Functionalization (CHE-1700982) D.G.M. gratefully acknowledges NSF  
272 MRI-R2 grant (CHE-0958205) and the use of the resources of the Cherry Emerson

273 Center for Scientific Computation. NMR and X-ray Instrumentation used in this work  
274 was supported by the National Science Foundation (CHE 1531620 and CHE 1626172).

275

276 **Author Contributions:** J.F. performed the synthetic experiments. Z.R. and J.M  
277 conducted the computational studies. J.B. conducted the X-ray crystallographic studies.  
278 J.F. and H.M.L.D. designed and analyzed the synthetic experiments and prepared the  
279 manuscript.

280

281 **Fig. 1 Background on C–H functionalization of unactivated alkanes and relationship to current**  
282 **work.** **a**, functionalization of cyclohexanes with donor/acceptor carbenes. We have previously described  
283 the asymmetric C–H functionalization of cyclohexane using catalyst **1**. In this work we show that the new  
284 catalyst **5** is capable of functionalizing the C-3 equatorial C–H bond of substituted cyclohexanes, leading  
285 to a stereoselective desymmetrization process. Ar = aryl or heteroaryl. **b**, illustration of the structure and  
286 challenge of functionalization of *tert*-butyl cyclohexane. **c**, optimization using the model substrate  
287 indicates that **5** can catalyze the functionalization of *tert*-butyl cyclohexane in a highly regioselective  
288 manner. See Supplementary Information Section 4 for experimental details and relevant spectra. Ar = (p-  
289 Br)C<sub>6</sub>H<sub>4</sub>, R = CO<sub>2</sub>CH<sub>2</sub>CCl<sub>3</sub>.

290

291 **Fig. 2 Scope of the reaction with respect to substrates and aryl diazoacetates.** Simple cycloalkanes  
292 were readily functionalized with good yield and high enantioselectivity. For substituted cyclohexane  
293 substrates, high site selectivity is routinely observed, resulting in C-3 insertion via a desymmetrization  
294 event, although diastereoselectivity is lower when the size of the substituent is small. The scope of  
295 aryl diazoacetates was broad, but sterically bulky *para*-substituents can lower enantioselectivity, as  
296 illustrated in compounds **33** and **34**. Heteroaryl donor groups were also compatible with this chemistry, as  
297 indicated by **36–38**. **a**: No ring diastereomers were observed. Abbreviations: r.r., regioisomeric ratio; d.r.,  
298 diastereomeric ratio; e.e., enantiomeric excess.

299

300 **Fig. 3 Functionalization of disubstituted cyclohexanes.** **a**, C–H functionalization of disubstituted  
301 cyclohexanes is more challenging, and the selectivity is governed by catalyst influence and subtle  
302 electronic preference of certain C–H bonds. Products were generally formed with high site- and  
303 stereoselectivity, although in a few cases d.r. is lower due to reaction with both enantiomeric chair forms.  
304 **a**: No ring diastereomers were observed. **b**: Due to symmetry, there are no side chain diastereomers. **b**, A  
305 substrate competition study indicated that the equatorial C–H bond reacted 140 times faster than its axial  
306 counterpart, illustrating the general steric influence of the rhodium carbene complex.

307

308 **Fig. 4 Rationalization of observed selectivities.** **a**, top view of the crystal structure and the illustrative  
309 view of the helicity of the phenyl groups; **b**, two calculated and energetically most stable isomers (**47a** and  
310 **47b**) of the catalyst. Isomer **47a** was optimized based on X-ray data; **c**, illustration of color-coding of  
311 atoms in carbene and *tert*-butyl cyclohexane in the calculated structures: donor group of carbene (blue),  
312 acceptor group of carbene (green), *tert*-butyl group of the substrate (red); **d**, calculated Rh-carbene  
313 complexes. Energetically, carbene binding to the top face (**48b**) is strongly favored over binding to the  
314 bottom face (**48a**); **e**, calculated lowest energy Rh-(carbene)(substrate) complex **49**. The atoms are color-  
315 coded according to default setting of Mercury: rhodium (blue), oxygen (red), hydrogen (white), carbon  
316 (grey). The highlighted atoms are marked according to the direction the phenyl group rotated: the phenyl  
317 groups in *M* helicity are marked light blue, and the ones in *P* helicity are marked pink.

318

319 **Supplementary Information is available in the online version of the paper.**

320

321 **Data Availability:** Crystallographic data for the structures reported in this Letter have  
322 been deposited at the Cambridge Crystallographic Data Centre, under deposition  
323 number CCDC 1855619, 1855620 and 1855295. Copies of the data can be obtained  
324 free of charge via [www.ccdc.cam.ac.uk/data\\_request/cif](http://www.ccdc.cam.ac.uk/data_request/cif). Complete experimental  
325 procedures and compound characterization data are available in the Supplementary  
326 Information, or from the corresponding author upon request.

327

328 Any correspondence and requests for materials should be addressed to H.M.L.D.

329

330 The authors have no competing financial interests.

331

332

333

334

335

336

337

338

339

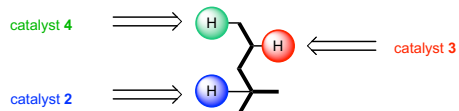
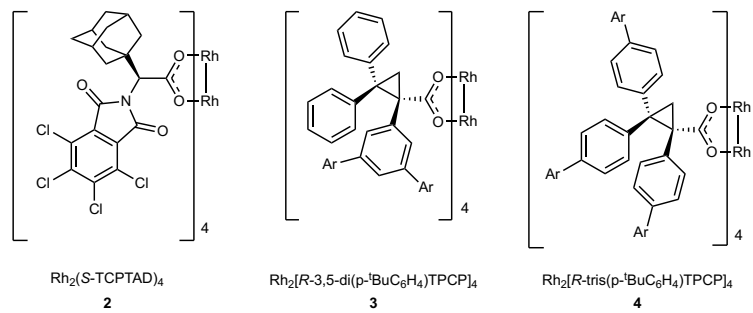
340

341

342

343

344



345  
346  
347  
348  
349

**Extended Data Fig. 1 Structures of previously established catalysts.** We have previously shown that through catalyst-directed C–H functionalization, we were able to selectively functionalize the most accessible primary, secondary and tertiary C–H bonds within a linear alkane substrate by using catalyst **2**, **3**, or **4**.